CARBON NANOPARTICLE FLOW BEHAVIOR NEAR RESPIRATORY MUCUS

Christin Grabinski, University of Dayton, 300 College Park, Dayton, OH 45469-0168, USA

Shadab Shaikh, University of Dayton, 300 College Park, Dayton, OH 45469-0168, USA

Khalid Lafdi, University of Dayton, 300 College Park, Dayton, OH 45469-0168, USA

Abstract

A numerical study was carried out to study the interaction of nanoparticles within the respiratory system. The respiratory tract is protected by a layer of mucus, which traps inhaled particles and bacteria. There have been many studies which have modeled the deposition of nanoparticles in the respiratory tract; however, few have taken into account the properties of respiratory mucus. In this study, the mucus layer was modeled as a porous media, and the Lagrangian multiphase approach was implemented in computational fluid dynamics software (CFD). A detailed parametric study was performed to predict the deposition of carbon nanoparticles on the mucus layer. Interfacial tension caused by a temperature difference between inhaled air and mucus was found to play a significant role in nanoparticle deposition. This study revealed that deposition increased with increasing temperature difference between inhaled air and mucus, as well as with the surface tension of the mucus. Nanoparticle deposition decreased with increasing inhaled air velocity and NP diameter. The results of this study confirm that respiratory mucus may play an important role in nanoparticle deposition.

Introduction

The growing field of nanotechnology has recently heightened concern regarding the impact of nanoparticles (NP) on human health. These concerns have been verified by epidemiological studies, which have reported an association between increased concentration of ambient NPs and respiratory illness and mortality (Peters and Wichmann, 2000). As new nano-devices and ideas develop, our environmental exposure to NPs continues to increase, and it is important to understand the interaction of NPs within the respiratory system. Carbon NPs are specifically of concern because they are formed in existing processes and have been proposed for use in many future applications. Combustion-derived NPs have been found to cause oxidative stress, inflammation, and cancer after inhalation (Donaldson et al., 2005). Also carbon NPs are adsorbent and can carry toxic chemicals into the respiratory system (Jakab et al., 1996).

Much of the respiratory tract is protected by a layer of mucus with functions of trapping inhaled particles and bacteria and acting as a diffusion barrier for deposited particles and gaseous air pollutants. Due to homeostasis, mucus composition, and therefore its rheological properties are continuously varying. One study suggests that diesel exhaust NPs can increase mucus secretion (Kobayashi and Ito, 1995), which could potentially alter the defense functions of mucus. It is important to understand NP deposition in the mucus layer for altered mucus properties.

Approaches to predicting NP deposition fall into two categories: computational and experimental. There have been several studies which have used computational models to simulate the deposition of NPs (Yu et al., 1996, Li et al., 1995, Zhang and Kleinstreuer 2004). Mitsakou et al. (2005) developed a Eularian model to study NP deposition in the lung and found that deposition of NPs to be exclusively by diffusion. Another study verified the transport and deposition of NPs via Brownian diffusion and found deposition efficiencies increased with decreasing NP size and lower inlet Reynolds numbers (Shi et al., 2004). Comparison of human and rat lung geometry in particle deposition patterns within asymmetric bronchial bifurcations found that interspecies differences play a major role in the deposition of NPs (Hofmann et al., 1996). The effect of airway mucus on NP deposition was not considered in any of these computational models.

In general, experimental studies have found that deposition efficiency of NPs decreases with increasing particle size and flow rate (Cheng et al., 1995, Yeh et al., 1997). Trends in NP deposition found in replica cast studies have been verified by *in vivo* studies, except *in vivo* studies have found NP deposition

to have weak dependence on flow rate (Yeh et al., 1997, Swift and Strong, 1996). Most replica cast studies have not accounted for mucus; however, in one study, an attempt was made by flooding a silicone nose model with concentrated dish liquid detergent and acetone (Cohen et al., 1990). The final surface properties of this artificial mucus coating were not compared to physiological mucus.

In the present work a detailed numerical analysis was performed to study the effects of mucus properties on the deposition of NPs. The numerical procedure was implemented in computational fluid dynamic (CFD) software. The Lagrangian multiphase approach was used to predict the deposition of carbon NPs in the mucus through a detailed parametric study. Due to constant changes in mucus composition and water content, the flow behavior of NPs was predicted with varying mucus surface tension. In addition to this, the effects of NP diameter, and inhaled air temperature and velocity were analyzed.

Numerical formulation

2.1 Model Domain

To simulate the inhalation process, NP filled humidified air was injected near a sheet of porous mucus (Figure 1A). The mucus membrane was modeled as a two-dimensional matrix consisting of a square unit cell (Figure 1B). The fluid (NP filled air) was assumed to be Newtonian, incompressible, and laminar.

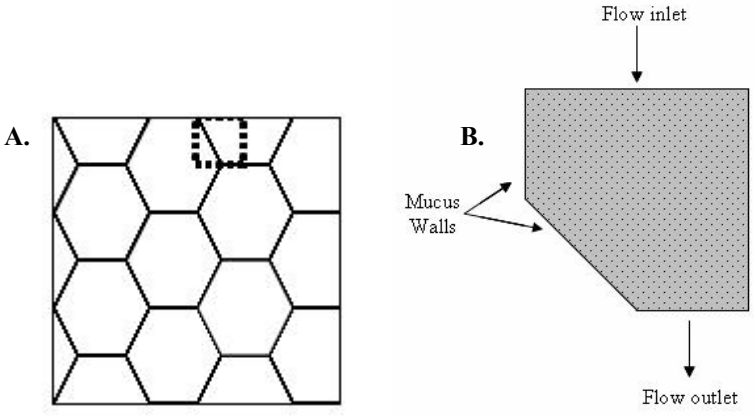

Figure 1. Model Domain
A. Porous mucus membrane; B. Representative

2.2 Model Parameters

The system parameters consisted of a humidified air stream filled with 10 nm diameter carbon NPs flowing at 1.5 m s^{-1} with mucus surface tension of 0.032 N m^{-1}. The velocity of inhaled NP filled air was based on literature values for resting inhalation flow rates and dimensions of the upper respiratory passage. At resting flowrate, air at room temperature of 295.15°K was warmed to 305.15°K after inhalation (Rouadi et al., 1999). The mucus wall temperature was assumed to be near physiological temperature (310.15°K). The dispersed spherical carbon NPs were presumed to be homogeneous in diameter.

2.3 Governing Equations

The governing equations include conservation of mass, momentum, and energy for two-dimensional geometry. A force balance was created on each NP including the effects of Brownian motion, Saffman's lift force, and drag force. For each parameter, the NP trajectories and the effect on maximum wall shear stress were predicted.

Continuity equation:

$$\nabla \vec{v} = 0 \tag{1}$$

where $\nabla \vec{v} = \frac{\partial v_x}{\partial x} + \frac{\partial v_y}{\partial y}$ and v_x and v_y are the fluid velocity components.

Momentum equation (for constant fluid viscosity and fluid density):

$$\rho_f(\vec{v}\nabla\vec{v}) = -\nabla p + \mu\nabla^2\vec{v} \tag{2}$$

where p is pressure, ρ_f is the fluid density, and μ is fluid viscosity.

The energy equation (for constant ρ_f and thermal conductivity):

$$\rho_f C_p\left[\frac{\partial}{\partial x}(Tv_x)+\frac{\partial}{\partial y}(Tv_y)\right] = k\left[\frac{\partial^2 T}{\partial x^2}+\frac{\partial^2 T}{\partial y^2}\right] \tag{3}$$

where C_p and k are the fluid specific heat and thermal conductivity respectively, and T is the fluid temperature.

2.3.1 Nanoparticle Trajectory

The equation of motion for a representative particle in the Lagrangian reference frame is taken by equating the particle inertia with the forces on the particle (Kleinstreuer, 2003):

$$\nabla\vec{v}_p = \left(\frac{18\mu}{{d_p}^2\rho_p C_c}\right)\nabla\cdot(\vec{v}-\vec{v}_p)+\frac{5.188\upsilon^{0.5}\rho_f\varepsilon_{ij}}{\rho_p d_p(\varepsilon_{lk}\varepsilon_{kl})^{0.25}}(v_j-v_{pj})+\zeta_i\sqrt{\frac{216\upsilon T}{\pi {d_p}^2{\rho_f}^{-1}{\rho_p}^2 C_c\Delta t}} \tag{4}$$

where $\vec{v}_p$ is the particle velocity, d_p is the particle diameter, ρ_p is the particle density, C_c is the Cunningham correction factor, ε_{ij} is the deformation rate tensor, and σ is the Stefan-Boltzmann constant. The first term in equation (4) is the drag force, the second term is the Saffman's Lift force due to shear, and the third term is the force of Brownian motion, modeled as a Gaussian white noise (Li and Ahmadi, 2002). The virtual mass force and the pressure force are neglected in the particle force balance equation because the density of the NPs is much greater than the fluid density. The trajectory calculations are based on the force balance on the particle, using the local continuous phase conditions as the particle moves through the flow.

Interfacial effects were included using the Marangoni stress to create a boundary condition describing the balance of stresses on the interface in order to solve for the wall shear stress in the momentum equation (coupled with the energy equation):

$$\tau = \frac{d\sigma}{dT}\nabla_s\cdot T \tag{5}$$

where $\frac{d\sigma}{dT}$ is the surface tension gradient with respect to temperature and $\nabla_s\cdot T$ is the surface gradient.

2.3 Numerical Solution

The momentum and heat exchanges from the continuous phase to the discrete phase were computed by examining the change in momentum and thermal energy of the NP as it passes through each control volume in the model. The NP phase is assumed sufficiently dilute that particle-particle interactions are negligible. The geometry for the mucus unit cell was modeled in GAMBIT software. The simulations for the analysis of NP deposition on the mucus wall were performed in FLUENT 6.2. When the NP makes contact with the wall, it is assumed to be trapped.

Results and Discussion

3.1 Validation of Numerical Technique

We verified the Lagrangian multiphase approach implemented in the present numerical study by comparing with the work of Elgafy and Lafdi (2006). The authors in their study used a two-dimensional simulation model based on Lagrangian multiphase approach for nanoparticle-filled fluid, which flows around an aligned microfiber matrix, to investigate and predict the nanoparticles trajectories and their interactions with fluid flow and microfiber walls. It was observed that the results from our numerical simulation for trajectory of nanoparticle flow showed a good agreement with the work of Elgafy and Lafdi, which was supportive of the numerical approach we adopted.

3.2 Parametric study

To analyze the effect of different system parameters on deposition, NPs were introduced into the system, and their flow behavior near mucus walls was predicted for several parameters. The system parameters consisted of an air stream filled with 10 nm diameter carbon NP and 100 % humidity flowing at 1.5 m s^{-1} with mucus surface tension of 0.032 N m^{-1}. For each study, one parameter was adjusted and the rest were held constant. The NPs were injected from the top wall of the unit cell close to the left boundary.

3.2.1 Effect of Inlet Air Velocity

The NP-filled air velocity was varied from 1-3.5 ms^{-1}. As expected, the maximum shear stress on the mucus walls increased with the increase in air velocity (Figure 3) causing a deviation in the flow of NPs away from the mucus wall (Figure 2). At low velocities, particle share more time in the vicinity of mucus walls, thus enhancing diffusional collection. As flow rate increases for constant diameter of particles in the micrometer range, the particle deposition increases (Kesavanathan and Swift, 1998).

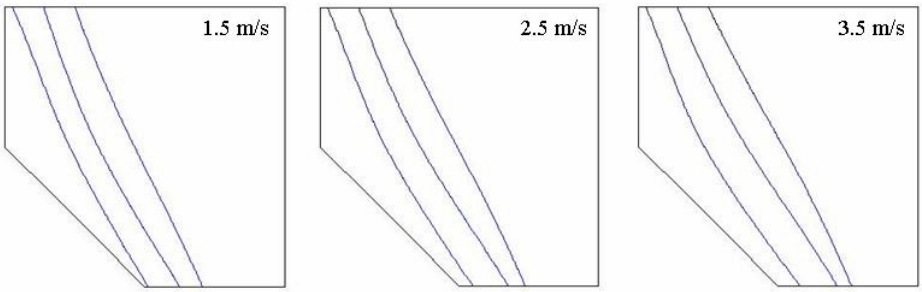

Figure 2. NPs flow near mucus walls for change in inlet velocity

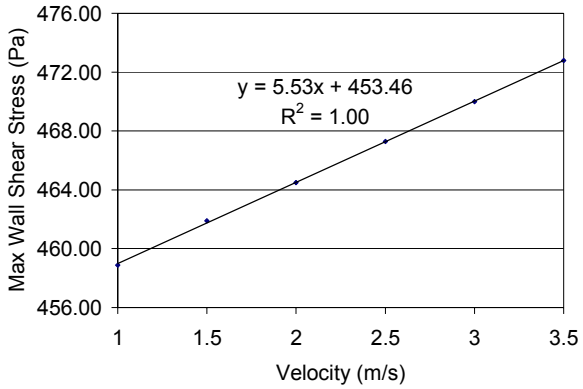

Figure 3. Variation of maximum shear stress for mucus wall with surface tension

3.2.2 Effect of NP Size

In the second case the NP diameter was varied from 2-50 nm. It was observed that NPs moved away from the mucus wall with the increase in their diameter (Figure 4). A similar trend was found in a replica cast study where nasal deposition for particles smaller than 0.04 μm increased with decreasing particle size (Cheng et al., 1995). Brownian motion increases for decreasing particle size; therefore, the diffusive deposition of particles is increased when the particle size is reduced. In the micrometer range, deposition is known to increase for increasing particle size (Kobayashi and Ito, 1995), which is due to the fact that deposition due to impaction increases as particle size increases.

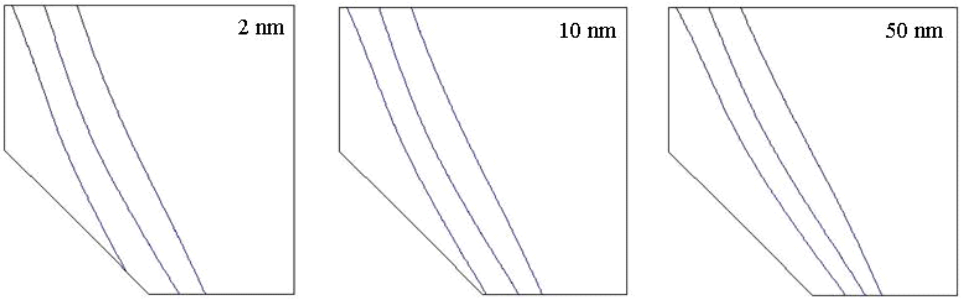

Figure 4. NPs flow near mucus walls for change in NP diameter

3.2.3 Effect of Inlet Air Mucus Wall Temperature Gradient

In the first study, the temperature difference between the NP-filled air and mucus walls was varied in the range 0-12°K by changing the inlet air temperature from 298.15-308.15 ° K. It was observed that the NPs were more attracted to the mucus wall with the decrease in the temperature gradient (Figure 5). This was due to the maximum wall shear stress which increased linearly with increase in the temperature gradient (Figure 6). NP deposition along the mucus wall (left wall of unit cell) could be mainly due to Brownian diffusion; however, interfacial effects would cause NPs to stick to the mucus layer.

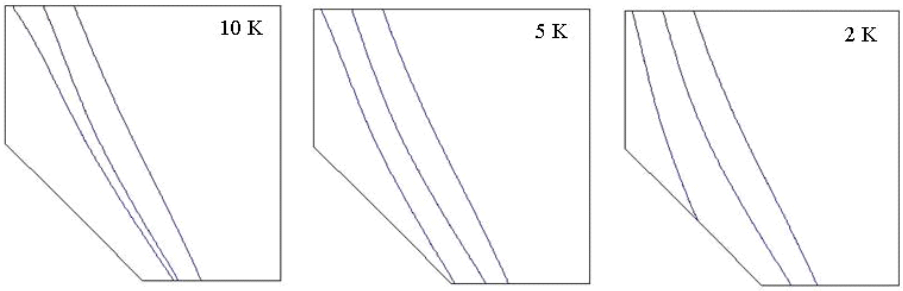

Figure 5. NP flow near mucus walls for change in temperature difference between the inhaled air and mucus walls

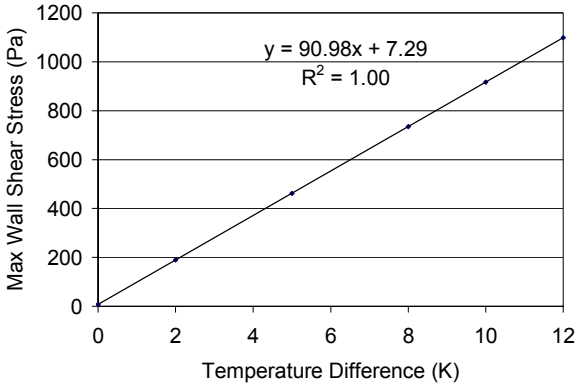

Figure 6. Variation of maximum shear stress for mucus wall with temperature gradient

3.2.4 Effect of Surface Tension

In the second case the surface tension of mucus wall was varied from 0.020-0.040 N m^{-1}. It was observed that by increasing the surface tension value NPs had an increased tendency to become trapped on the mucus walls (Figure 7). This was attributed to the change in the maximum wall shear stress which is related to the surface tension gradient and decreased linearly with increase in the wall surface tension (Figure 8). From the practical point of view, the capillary effects due to the increase in surface tension would cause the air stream to be pulled towards the mucus wall and hence the deposition of NPs on its surface.

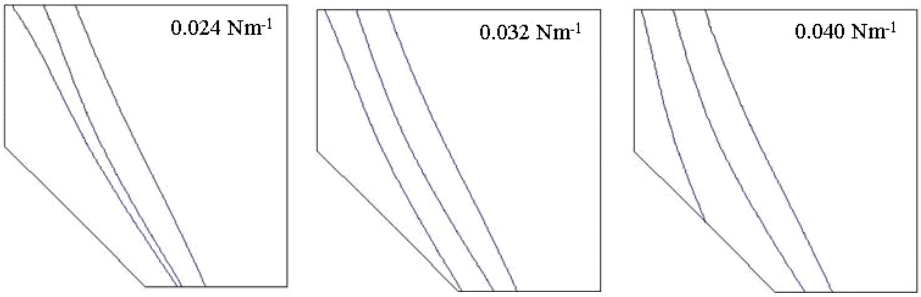

Figure 7. NPs flow near mucus walls for change in surface tension

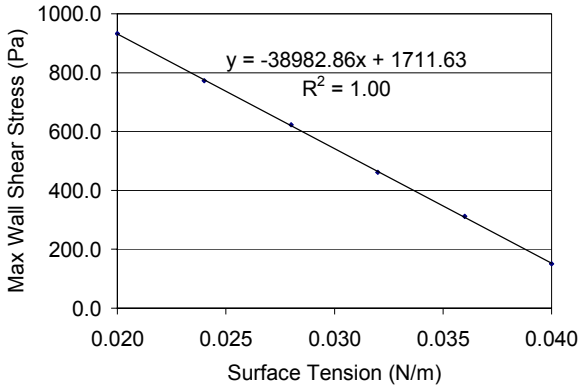

Figure 8. Variation of maximum shear stress for mucus wall with surface tension

Conclusion

Numerical simulations were carried out to study the deposition of NPs flowing with air stream through the respiratory mucus cavity. The numerical procedure was implemented in CFD software using the Lagrangian multiphase approach. A parametric study was carried out to analyze the effects of different parameters, namely; inlet air temperature and velocity, mucus wall surface tension, and NP diameter on the deposition of NPs on the mucus wall. The study revealed that the NPs had a greater tendency for deposition with increase in surface tension of mucus wall. On the other hand with the increase in air flow velocity, air-mucus wall temperature gradient and NP diameter the NPs moved away from the mucus wall. The results from this study emphasized the significance of respiratory mucus layer in the trapping of NPs under different conditions encountered in the flow through the respiratory passage. The feedback from the current study will be used to perform experimental investigations to have a better insight on the role played by the mucus membrane in NP deposition in the respiratory passage.

References

Cheng, Y.S., S.M. Smith, H.C. Yeh, D.B Kim, K.H. Cheng and D.L. Swift. 1995. Deposition of ultrafine aerosols and thoron progeny in replicas of nasal airways of young children. *Aerosol Science and Technology* 23:541-552.

Cohen, B.S., R.G. Sussman and M. Lippman. 1990. Ultrafine Particle Deposition in a Human Tracheobronchial Cast. *Aerosol Science and Technology* 12:1082-1091.

Donaldson, K., L. Tran, L. Jimenez, R. Duffin, D. Newby, N. Mills, W. MacNee and V. Stone. 2005. Combustion-derived nanoparticles: A review of their toxicology following inhalation exposure. *Particle and Fibre Toxicology.* 2:10.

Elgafy, A. and K. Lafdi. 2006. Engineering solution in monitoring nanoparticle-fluid flow during nanocomposites processing**.** *Journal of Nanoparticle Research* 2006.

Hofmann, W., I. Balashazy, T. Heistracher and L. Koblinger. 1996. The significance of particle deposition patters in bronchial airway bifurcations for extrapolation modeling. *Aerosol Science and Technology* 25:305-327.

Jakab, G.J., R.W. Clarke, D.R. Hemenway, M.V. Longphre, S.R. Kleeberger and R. Frank. 1996. Inhalation of acid coated carbon black particles impairs alveolar macrophage phagocytosis. *Toxicology Letters* 88:243-248.

Kesavanathan, J. and D.L. Swift. 1998. Human nasal passage particle deposition: the effect of particle size, flow rate, and anatomical factors. *Aerosol Science and Technology* 28:457–463.

Kleinstreuer, C. 2003. Two-phase Flow. Taylor & Frances, New York 133-226.

Kobayashi, T. and T. Ito. 1995. Diesel exhaust particulates induce nasal mucosal hyperresponsiveness to inhaled histamine aerosol. *Fundamental and Applied Toxicology* 27:195-202.

Li, A. and G. Ahmadi. 1995. Computer simulation of particle deposition in the upper tracheobronchial tree. *Aerosol Science and Technology* 23:201-223.

Li, A. and G. Ahmadi. 1992. Dispersion and deposition of spherical particles from point sources in a turbulent channel flow. *Aerosol Science and Technology* 16:209-226.

Mitsakou, C., C. Helmis, and C. Housiadas. 2005. Eulerian modelling of lung deposition with sectional representation of aerosol dynamics. *Journal of Aerosol Science* 36:75-94.

Peters, A. and H.E. Wichmann. 2000. Epidemiological evidence of the effects of ultrafine particle exposure. *Philosophical Transactions of the Royal Society of London, Series A* 358:2751–2769.

Rouadi, P., F.M. Baroody, D. Abbott, E. Naureckas, J. Solway and R.M. Naclerio. 1999. A technique to measure the ability of the human nose to warm and humidify air. *Journal of Applied Physiology* 87:400-406.

Shi, H., C. Kleinstreuer, and Z. Zhang. 2004. Nanoparticle transport and deposition in bifurcating tubes with different inlet conditions. *Physics of Fluids* 16:2199-2213.

Swift, D.L. and J.C. Strong. 1996. Nasal deposition of ultrafine ^{218}Po aerosols in human subjects. *Journal of Aerosol Science* 27:1125-1132.

Yeh, H.C., B.A. Muggenburg, J.R. Harkema. 1997. *In vivo* deposition of inhaled ultrafine particles in the respiratory tract of rhesus monkeys. *Aerosol Science and Technology* 27(4):465-470.

Yu, G., Z. Zhang, and R. Lessmann. 1996. Computer simulation of the flow field and particle deposition by diffusion in a 3-D human airway bifurcation. *Aerosol Science and Technology* 25:338-352.

Zhang, Z. and C. Kleinstreuer. 2004. Airflow structures and nano-particle deposition in a human upper airway model. *Journal of Computational Physics* 198:178–210**.**